Centrum voor Wiskunde en Informatica

REPORT*RAPPORT*

MAS

Modelling, Analysis and Simulation

Modelling, Analysis and Simulation

Exact Riemann solver for RMHD in the case of shocks only

D.E.A. van Odyck

REPORT MAS-E0501 JANUARY 2005

CWI is the National Research Institute for Mathematics and Computer Science. It is sponsored by the Netherlands Organization for Scientific Research (NWO).
CWI is a founding member of ERCIM, the European Research Consortium for Informatics and Mathematics.

CWI's research has a theme-oriented structure and is grouped into four clusters. Listed below are the names of the clusters and in parentheses their acronyms.

Probability, Networks and Algorithms (PNA)

Software Engineering (SEN)

Modelling, Analysis and Simulation (MAS)

Information Systems (INS)

P.O. Box 94079, 1090 GB Amsterdam (NL)
Kruislaan 413, 1098 SJ Amsterdam (NL)
Telephone +31 20 592 9333
Telefax +31 20 592 4199

ISSN 1386-3703

Exact Riemann solver for RMHD in the case of shocks only

ABSTRACT
In this paper the quasi-1D relativistic magneto-hydrodynamic (RMHD) equations are numerically solved with a Lax-Friedrichs scheme. The RMHD shock relations are studied in detail. An ansatz is made to build an exact Riemann solver for RMHD. The results of the exact Riemann solver are compared with the numerical solutions of the Lax-Friedrichs scheme.

2000 Mathematics Subject Classification: 65M60, 76L05, 76Nxx, 76Y05, 83A05, 85A30
Keywords and Phrases: special relativity, magneto-hydrodynamics, Riemann problems.
Note: This research was supported by the Netherlands Organization for Scientific Research (NWO). The work was carried out under CWI-project MAS2.1 "Computational Fluid Dynamics and Computational Electromagnetics".

Exact Riemann solver for RMHD
in the case of shocks only

D.E.A. van Odyck
CWI
P.O. Box 94079, 1090 GB Amsterdam, The Netherlands

ABSTRACT
In this paper the quasi-1D relativistic magneto-hydrodynamic (RMHD) equations are numerically solved with a Lax-Friedrichs scheme. The RMHD shock relations are studied in detail. An ansatz is made to build an exact Riemann solver for RMHD. The results of the exact Riemann solver are compared with the numerical solutions of the Lax-Friedrichs scheme

2000 Mathematics Subject Classification: 65M60, 76L05, 76Nxx, 76Y05, 83A05, 85A30
Keywords and Phrases: special relativity, magneto-hydrodynamics, Riemann problems.
Note: This research was supported by the Netherlands Organization for Scientific Research (NWO). The work was carried out under CWI-project MAS2.1 "Computational Fluid Dynamics".

1. Theory RMHD

In this section a summary is given of the equations describing the flow of a relativistic flowing plasma. In the following we set the light speed to unity, $c = 1$. This corresponds to the scaling:

$$\begin{pmatrix} \mathbf{v} \\ p \\ \epsilon' \\ \mathbf{E} \\ \mathbf{B} \\ t \end{pmatrix} \rightarrow \begin{pmatrix} \mathbf{v}c \\ pc^2 \\ \epsilon' c^2 \\ \mathbf{E}c \\ \mathbf{B}c \\ t/c \end{pmatrix} , \tag{1.1}$$

where $\mathbf{v}$ represents the velocity vector, p the pressure, ϵ' the internal energy density, $\mathbf{E}$ the electric field vector, $\mathbf{B}$ the magnetic field vector and t the time. In ideal MHD it is assumed that the conductivity is infinite: $\sigma = \infty$. Therefore the expression for the current

$$\frac{\mathbf{j}}{\sigma} = \frac{\rho^e}{\sigma}\mathbf{v} + \mathbf{E} + \mathbf{v} \times \mathbf{B} , \tag{1.2}$$

where ρ^e is the charge density, reduces to:

$$\mathbf{E} = -\mathbf{v} \times \mathbf{B} . \tag{1.3}$$

So, in the fluid's rest ($\mathbf{v} = 0$) frame: $\mathbf{E} = 0$. In general, the electromagnetic field can be written in the compact form:

$$\frac{\partial \tilde{F}^{\mu\nu}}{\partial x^\nu} = 0 \rightarrow \begin{cases} \nabla \cdot \mathbf{B} = 0 \\ \frac{\partial \mathbf{B}}{\partial t} + \nabla \times \mathbf{E} = 0 \end{cases} , \tag{1.4}$$

$$\frac{\partial F^{\mu\nu}}{\partial x^\nu} = -j^\mu \rightarrow \begin{cases} \nabla \cdot \mathbf{E} = \rho^e \\ -\frac{\partial \mathbf{E}}{\partial t} + \nabla \times \mathbf{B} = \mathbf{j} \end{cases} , \tag{1.5}$$

where $j^\mu = (\rho^e, \mathbf{j})$ and

$$\tilde{F}^{\mu\nu} = \begin{bmatrix} 0 & -B_x & -B_y & -B_z \\ B_x & 0 & E_z & -E_y \\ B_y & -E_z & 0 & E_x \\ B_z & E_y & -E_x & 0 \end{bmatrix} . \tag{1.6}$$

The tensor $\tilde{F}^{\mu\nu}$ is the dual of $F^{\mu\nu}$. They are connected through the relations: $\tilde{F}^{\mu\nu} = \frac{1}{2}\epsilon^{\mu\nu\rho\sigma}F_{\rho\sigma}$ and $F^{\mu\nu} = \frac{1}{2}\epsilon^{\mu\nu\rho\sigma}\tilde{F}_{\rho\sigma}$ and $\epsilon^{\mu\nu\rho\sigma}$ is the Levi-Civita alternating symbol.

In the fluid's rest frame ($\mathbf{E}' = 0$) we have:

$$\tilde{F}^{\mu\nu}_{rest} = \begin{bmatrix} 0 & -B'_x & -B'_y & -B'_z \\ B'_x & 0 & 0 & 0 \\ B'_y & 0 & 0 & 0 \\ B'_z & 0 & 0 & 0 \end{bmatrix} . \tag{1.7}$$

This can be written in another form like:

$$\tilde{F}^{\mu\nu}_{rest} = b^\mu_{rest}u^\nu_{rest} - b^\nu_{rest}u^\mu_{rest} , \tag{1.8}$$

where $u^\mu_{rest} = (1,0,0,0)$ and $b^\mu_{rest} = (0, \mathbf{B}')$. A general Lorentz transformation $(\Lambda^\mu{}_\nu)$ is used to transform to the laboratory (LAB) frame:

$$\tilde{F}^{\mu\nu} = \Lambda^\mu{}_\alpha\Lambda^\nu{}_\beta(b^\alpha_{rest}u^\beta_{rest} - b^\beta_{rest}u^\alpha_{rest}) . \tag{1.9}$$

In the LAB-frame we have:

$$u^\nu = \Lambda^\nu{}_\beta u^\beta_{rest} = (\Gamma, \Gamma\mathbf{v}) , \tag{1.10}$$

where $\Gamma = 1/\sqrt{(1 - \mathbf{v}\cdot\mathbf{v})}$ is the Lorentz factor and

$$b^\mu = \Lambda^\mu{}_\alpha b^\alpha_{rest} = \left((\mathbf{v}\cdot\mathbf{B}')\Gamma, \mathbf{B}' + (\Gamma - 1)\frac{(\mathbf{v}\cdot\mathbf{B}')}{(\mathbf{v}\cdot\mathbf{v})}\mathbf{v}\right) . \tag{1.11}$$

In general, the magnetic field transforms under a Lorentz transformation like:

$$\mathbf{B}' = \Gamma(\mathbf{B} - \mathbf{v}\times\mathbf{E})) - (\Gamma - 1)\frac{(\mathbf{v}\cdot\mathbf{B})}{(\mathbf{v}\cdot\mathbf{v})}\mathbf{v} . \tag{1.12}$$

We can use equation (1.12) and the MHD condition $\mathbf{E} = -\mathbf{v}\times\mathbf{B}$ to simplify the expression for b^μ

$$b^\mu = \left((\mathbf{v}\cdot\mathbf{B})\Gamma, \frac{\mathbf{B}}{\Gamma} + \Gamma(\mathbf{v}\cdot\mathbf{B})\mathbf{v}\right) . \tag{1.13}$$

In general the energy-momentum tensor for the electromagnetic field looks like:

$$T^{\mu\nu}_{EM} = F^\mu{}_\beta F^{\beta\nu} + \frac{1}{4}F_{\alpha\beta}F^{\alpha\beta} = -\frac{1}{4}g^{\mu\nu}\tilde{F}_{\xi\eta}\tilde{F}^{\xi\eta} - g^{\mu\lambda}\tilde{F}_{\lambda\eta}\tilde{F}^{\eta\nu} , \tag{1.14}$$

where $g^{\mu\nu} = diag(-1,1,1,1)$ is the Minkowski metric. After substitution of equation (1.9) one finds:

$$T^{\mu\nu}_{EM} = |b|^2\left(u^\mu u^\nu + \frac{1}{2}g^{\mu\nu}\right) - b^\mu b^\nu , \ |b|^2 = b_\xi b^\xi . \tag{1.15}$$

This energy-momentum tensor can be combined with the energy-momentum tensor for the fluid motion, derived in Odyck [9]:

$$T^{\mu\nu}_{HD} = (e+p)u^\mu u^\nu + pg^{\mu\nu} , \ e = \rho + \epsilon' , \tag{1.16}$$

where ρ is the rest mass density. The energy-momentum conservation of the RMHD fluid without external sources is now described by:

$$\nabla_\nu T^{\mu\nu} = 0 \ , \ T^{\mu\nu} = T^{\mu\nu}_{HD} + T^{\mu\nu}_{EM} \ . \tag{1.17}$$

The Maxwell equations in the ideal MHD approximation now read:

$$\frac{\partial \tilde{F}^{\mu\nu}}{\partial x^\nu} = \frac{\partial}{\partial x^\nu}(b^\mu u^\nu - b^\nu u^\mu) = 0 \rightarrow \left\{ \begin{array}{l} \nabla \cdot \mathbf{B} = 0 \\ \frac{\partial \mathbf{B}}{\partial t} - \nabla \times (\mathbf{v} \times \mathbf{B}) = 0 \end{array} \right. \ . \tag{1.18}$$

These are the same as in MHD. To the above equations (1.17),(1.18) we add: the continuity equation,

$$\nabla_\mu (\rho u^\mu) = 0 \ , \tag{1.19}$$

the state equation (ideal gas law),

$$e + p = \rho + \frac{\gamma}{\gamma - 1} p \ , \tag{1.20}$$

and some initial conditions.

The system of equations (1.17), (1.18) and (1.19) consists of ten unknowns (u^μ, b^μ, p, ρ) and nine equations. To analyze the RMHD equations Anile [1] adds an equation for the entropy and writes the system in quasi-linear form:

$$A^{\alpha A}_B \nabla \bar{U}^B = 0 \ , \quad A, B = 0, ..., 9 \ , \tag{1.21}$$

where $\bar{U} = (u^\mu, b^\mu, p, S)$ and S the entropy. For the explicit form of $A^{\alpha A}_B \nabla$ and an in depth analysis of this system see Anile [1], Section 2.4. The following variables are defined:

$$a = u_\mu \phi^\mu \ , \ B = b_\mu \phi^\mu \ , \ H = \phi_\mu \phi^\mu \ , \ e'_p = \frac{\partial e(p,S)}{\partial p} \ , \ \eta = e + p \ , \ E = \eta + |b|^2 \ . \tag{1.22}$$

and in the case where the waves propagate in the x-direction with a speed λ, the normal to the characteristic hyper-surface is given by:

$$\phi^\mu = \Gamma(\lambda)(\lambda, 1, 0, 0) \ , \ \Gamma(\lambda) = \frac{1}{\sqrt{1 - \lambda^2}} \ . \tag{1.23}$$

In Anile [1], Section 2.4, it is shown that the system of equations (1.21) is hyperbolic in time and can be characterized by the following eigenvalues:

- The entropy wave:

$$\lambda_e = v_x \ . \tag{1.24}$$

- The Alfvén wave:

$$Ea^2 - B^2 = 0 \ , \text{ with two solutions } \lambda^\pm_A. \tag{1.25}$$

- The fast and slow magneto-acoustic waves:

$$\eta(e'_p - 1)a^4 + (-(\eta + e'_p|b|^2)a^2 + B^2)\phi^\mu \phi_\mu = 0 \ , \text{ with four solutions } \lambda^\pm_f, \lambda^\pm_s. \tag{1.26}$$

- The characteristic wave speeds are ordered in the same way as in MHD:
$-1 < \lambda^-_f \leq \lambda^-_A \leq \lambda^-_s \leq \lambda_e \leq \lambda^+_s \leq \lambda^+_A \leq \lambda^+_f < 1$.

The corresponding right eigenvectors can be calculated and are given in Anile [1]. In the following we are especially interested in the one-dimensional case. The RMHD equations can then be put in the form:

$$\frac{\partial \mathbf{U}}{\partial t} + \frac{\partial \mathbf{F}(\mathbf{U})}{\partial x} = 0 \ , \tag{1.27}$$

with

$$\mathbf{U} = \begin{pmatrix} \Gamma\rho \\ (\rho h + |b|^2)\Gamma^2 v_x + b_0 b_x \\ (\rho h + |b|^2)\Gamma^2 v_y + b_0 b_y \\ (\rho h + |b|^2)\Gamma^2 v_z + b_0 b_z \\ (\rho h + |b|^2)\Gamma^2 - (p + |b|^2/2) - b_0^2 \\ B_y \\ B_z \end{pmatrix} \ , \ \mathbf{F}(\mathbf{U}) = \begin{pmatrix} \Gamma\rho v_x \\ (\rho h + |b|^2)\Gamma^2 v_x^2 + (p + |b|^2/2) - b_x^2 \\ (\rho h + |b|^2)\Gamma^2 v_x v_y - b_x b_y \\ (\rho h + |b|^2)\Gamma^2 v_x v_z - b_x b_z \\ (\rho h + |b|^2)\Gamma^2 v_x + b_0 b_x \\ B_y v_x - B_x v_y \\ B_z v_x - B_x v_z \end{pmatrix} , \tag{1.28}$$

where $h = (e+p)/\rho$ is the enthalpy. The eigenvalues of $\frac{\partial \mathbf{F}(\mathbf{U})}{\partial \mathbf{U}}$ are still given by equations (1.24), (1.25) and (1.26) and the right eigenvectors can be found after some rearrangements of the eigenvectors of system (1.21), see Balsara [2].

2. Shock relations

A way to calculate the shock curve is to follow the procedure given in Majorana [7]. From equations (1.17), (1.18) and (1.19) we obtain the jump conditions for RMHD:

$$\begin{array}{l} [\rho u^\mu]\, l_\mu = 0 \ , \\ [b^\mu u^\nu - u^\mu b^\nu]\, l_\mu = 0 \ , \\ [T^{\mu\nu}]\, l_\mu = 0 \ , \end{array} \tag{2.1}$$

where l^μ is the four-vector normal to the shock hyper-surface and $[f] = f_+ - f_-$ with f_- (f_+) the quantity f before (after) the shock. For a shock propagating along the x-axis in the LAB-frame $l^\mu = \Gamma(v_s)(v_s, 1, 0, 0)$ and v_s is the shock speed in the LAB-frame. The shock relations can be rewritten in the form:

$$\begin{array}{l} [\rho a] = 0 \ , \\ [B u^\mu - a b^\mu] = 0 \ , \\ \left[(e + p + |b|^2) u^\mu a + (p + \frac{1}{2}|b|^2) l^\mu - B b^\mu\right] = 0 \ , \end{array} \tag{2.2}$$

where the definitions for a and B are used but now with ϕ^μ replaced by l^μ. The shock relations can be solved in different ways, corresponding to different discontinuities.

- Contact discontinuity $m = \rho a = 0$.

$$[a] = 0 \ , \quad [B] = 0 \ , \quad [|b|^2] = 0 \ , \quad [u^\mu] = 0 \ , \quad [b^\mu] = 0 \ , \text{resulting in } [p] = 0 \ , \quad [\rho] \neq 0 \ .$$

- Tangential discontinuity $m = \rho a = 0$ and $B_- = B_+ = 0$. Then only:

$$[p + \frac{1}{2}|b|^2] = 0 \ .$$

- Alfvén shock $m \neq 0$. In Lichnerowicz [6] pg. 161 the Alfvén shock is defined to be the case $\alpha_- = \alpha_+ = 0$ and $\alpha = (e + p + |b|^2)/\rho - B^2/m^2$. It is mentioned that the characteristic speed for the Alfvén wave follows from equation (1.25): $Ea^2 - B^2 = m^2\alpha = 0$. So, the Alfvén wave

speed before and after the Alfvén shock is the same. In Lichnerowicz [6] pg. 164 the following shock relations are deduced:

$$[p] = 0 \ , \ [\rho] = 0 \ , \ [|b|^2] = 0 \ , \ [a] = 0 \ , \ [B] = 0 \ , \ \left[\frac{e+p}{\rho}\right] = 0 \ .$$

- Slow and fast magneto-acoustic shocks $m \neq 0$, solve the shock relations (2.2).

We now try to solve the shock relations in the case of the slow and fast magneto-acoustic shocks. Introduce the following variables:

$$\rho G(z) = e + p \ , \quad \tilde{b}^\mu = b^\mu/\sqrt{\rho}_- \ , \quad \tilde{B} = \tilde{b}^\mu l_\mu \ , \quad a = u^\mu l_\mu \ , \quad n = \rho/\rho_- \ , \quad z = \rho/p \ , \tag{2.3}$$

where for an ideal gas $G(z) = 1 + \frac{\gamma}{\gamma-1}\frac{1}{z}$. The shock relations (2.2) can be rewritten in the form:

$$\begin{aligned} &[na] = 0 \ , \\ &\left[\tilde{B}u^\mu - a\tilde{b}^\mu\right] = 0 \ , \\ &\left[nGau^\mu + (\tfrac{n}{z})l^\mu + |\tilde{b}|^2(au^\mu + \tfrac{1}{2}l^\mu) - \tilde{B}\tilde{b}^\mu\right] = 0 \ , \end{aligned} \tag{2.4}$$

or in the form:

$$[M] = 0 \ , \quad [Q] = 0 \ , \quad [P] = 0 \ , \tag{2.5}$$

$$\left[aG + \frac{1}{az} + \frac{1}{2a^2}\left(Q + \frac{P^2}{G^2}\right)\right] = 0 \ , \tag{2.6}$$

$$\left[G^2(1+a^2) + 2\frac{Q}{a}\left(G - \frac{1}{z}\right) + 2\frac{P^2}{aG}\right] = 0 \ , \tag{2.7}$$

where

$$M = na \ , \quad MQ = a^2|\tilde{b}|^2 - \tilde{B}^2 \ , \quad \sqrt{M}P = BG \ . \tag{2.8}$$

It is noticed that these relations are frame invariant.

Equations (2.6) and (2.7) can be rewritten in two equations with two unknowns: a_+ and z_+.

$$f_0 = a_-G_- + \frac{1}{a_-z_-} + \frac{1}{2a_-^2}\left(\sigma_1 + \frac{\sigma_2}{G_-^2}\right) = a_+G_+ + \frac{1}{a_+z_+} + \frac{1}{2a_+^2}\left(\sigma_1 + \frac{\sigma_2}{G_+^2}\right) \ , \tag{2.9}$$

$$f_1 = G_-^2(1+a_-^2) + 2\frac{\sigma_1}{a_-}\left(G_- - \frac{1}{z_-}\right) + 2\frac{\sigma_2}{a_-G_-} = G_+^2(1+a_+^2) + 2\frac{\sigma_1}{a_+}\left(G_+ - \frac{1}{z_+}\right) + 2\frac{\sigma_2}{a_+G_+} \ , \tag{2.10}$$

where

$$\sigma_1 = \frac{a_-^2|\tilde{b}|_-^2 - \tilde{B}_-^2}{n_-a_-} \ , \quad \sigma_2 = \frac{\tilde{B}_-^2G_-^2}{n_-a_-} \ . \tag{2.11}$$

After some manipulations of the above equations they can be solved for a_+ as a function of z_+.

$$a_+^{(\pm)} = \frac{f_1 + \frac{G_+}{z_+} - G_+^2 \pm \sqrt{\left(f_1 + \frac{G_+}{z_+} - G_+^2\right)^2 - 4G_+f_0\left(\frac{3}{2}G_+\sigma_1 + \frac{3}{2}\frac{\sigma_2}{G_+} - 2\frac{\sigma_1}{z_+}\right)}}{2G_+f_0} \ . \tag{2.12}$$

The correct solution for a_+, $a_+^{(+)}$ or $a_+^{(-)}$, is found by back substitution of $a_+^{(\pm)}$ into equation (2.9) or (2.10).

In the following a_+ represents the correct solution $a_+^{(+)}$ or $a_+^{(-)}$. The ideal gas law is used:

$$G(z) = 1 + \bar{\gamma}\frac{1}{z} \ , \quad \bar{\gamma} = \frac{\gamma}{1-\gamma} \ . \tag{2.13}$$

To calculate a_+ we need z_+ in equation (2.12). In the following we are going to eliminate a_+ from equations (2.9) and (2.10). The equations (2.9) and (2.10) can be written in polynomial form.

$$\underbrace{(\bar{\gamma}+z_+)^3}_{a_3} a_+^3 + \underbrace{-f_0 z_+(\bar{\gamma}+z_+)^2}_{a_2} a_+^2 + \underbrace{(\bar{\gamma}+z_+)^2}_{a_1} a_+ +$$

$$+ \underbrace{\frac{1}{2} z_+(z_+^2\sigma_2 + \sigma_1(\bar{\gamma}+z_+)^2)}_{a_0} = 0 \ , \tag{2.14}$$

$$\underbrace{f_0 z_+(\bar{\gamma}+z_+)^2}_{b_2} a_+^2 + \underbrace{(\bar{\gamma}+z_+)((\bar{\gamma}+z_+)^2 - \bar{\gamma} - z_+(z_+ f_1 + 1))}_{b_1} a_+ +$$

$$+ \underbrace{\frac{1}{2} z_+(3z_+^2\sigma_2 + \sigma_1(\bar{\gamma}+z_+)(3\bar{\gamma}+3z_+-4))}_{b_0} = 0 \ . \tag{2.15}$$

The above equations can be reduced to one single polynomial equation in the unknown variable z_+.

To do so we follow the following procedure. If you want to find an x which is the solution of

$$f(x) = a_3 x^3 + a_2 x^2 + a_1 x + a_0 = 0 \ , \tag{2.16}$$

and at the same time a solution of

$$g(x) = b_2 x^2 + b_1 x + b_0 = 0 \ , \tag{2.17}$$

the coefficients of the above polynomials must satisfy a certain condition. Take

$$e(x) = b_2 f(x) - a_3 x g(x) = \underbrace{(b_2 a_2 - a_3 b_1)}_{c_2} x^2 + \underbrace{(b_2 a_1 - a_3 b_0)}_{c_1} x + \underbrace{b_2 a_0}_{c_0} \ , \tag{2.18}$$

then equations (2.16), (2.17) transform into

$$c_2 g(x) - b_2 e(x) = (c_2 b_1 - c_1 b_2)x + c_2 b_0 - c_0 b_2 = 0 \ , \tag{2.19}$$

$$b_1 e(x) - c_1 g(x) = (c_2 b_1 - c_1 b_2)x^2 + c_0 b_1 - c_1 b_0 = 0 \ . \tag{2.20}$$

Equation (2.19) is solved for x,

$$x = \frac{c_0 b_2 - c_2 b_0}{c_2 b_1 - c_1 b_2} \ . \tag{2.21}$$

This result is substituted in equation (2.20) and gives the existence condition for equations (2.16) and (2.17):

$$(c_2 b_1 - c_1 b_2)(c_1 b_0 - c_0 b_1) - (c_2 b_0 - c_0 b_2)^2 = 0 \ . \tag{2.22}$$

We can now substitute in equation (2.22) the expressions for a_i and b_i given in equations (2.14) and (2.15). This gives a polynomial of order eight in the variable z_+. It can be solved with a standard numerical scheme for solving polynomials in one variable (I use the NAG Fortran routine C02AGF. It uses a variant of Laguerre's method, see Smith [10]). The value for z_+ is used to calculate a_+ with equation (2.12). Also the other unknown quantities can now be calculated:

$$n_+ = \frac{a_-}{a_+} \ , \quad \tilde{B}_+ = \tilde{B}_- \frac{G_-}{G_+} \ , \quad |\tilde{b}|_+^2 = \frac{a_-^2 |\tilde{b}|_-^2 - \tilde{B}_-^2 + \tilde{B}_+^2}{a_+^2} \ . \tag{2.23}$$

In the subsection "Results" some typical solutions for n_+ and z_+ are presented.

2.1 Frames of reference

We can solve the shock relation independent of the frame of reference. Different frames can be used to calculate the input variables: the fluid's rest-frame ahead of the shock, the LAB-frame, the shock frame and the S-frame where the shock is stationary and $v_y^- = v_z^- = 0$. A general Lorentz transformation in the boost direction $\mathbf{u}$ looks like:

$$\Lambda^\mu{}_\nu = \begin{pmatrix} \Gamma & -u_x\Gamma & -u_y\Gamma & -u_z\Gamma \\ -u_x\Gamma & 1+(\Gamma-1)\frac{u_x^2}{\mathbf{u}\cdot\mathbf{u}} & (\Gamma-1)\frac{u_x u_y}{\mathbf{u}\cdot\mathbf{u}} & (\Gamma-1)\frac{u_x u_z}{\mathbf{u}\cdot\mathbf{u}} \\ -u_y\Gamma & (\Gamma-1)\frac{u_x u_y}{\mathbf{u}\cdot\mathbf{u}} & 1+(\Gamma-1)\frac{u_y^2}{\mathbf{u}\cdot\mathbf{u}} & (\Gamma-1)\frac{u_y u_z}{\mathbf{u}\cdot\mathbf{u}} \\ -u_z\Gamma & (\Gamma-1)\frac{u_x u_z}{\mathbf{u}\cdot\mathbf{u}} & (\Gamma-1)\frac{u_y u_z}{\mathbf{u}\cdot\mathbf{u}} & 1+(\Gamma-1)\frac{u_z^2}{\mathbf{u}\cdot\mathbf{u}} \end{pmatrix} \ , \ \Gamma = \frac{1}{\sqrt{(1-\mathbf{u}\cdot\mathbf{u})}} \ . \quad (2.24)$$

If the velocity 4-vector (u^μ), the magnetic 4-vector (b^μ) and the shock normal ($l^\mu = \Gamma(v_s)(v_s,1,0,0)$) are given in the LAB-frame, they can be transformed to the S-frame with first a boost in the shock direction ($\mathbf{u} = (v_s,0,0) \rightarrow \tilde{\Lambda}^\mu{}_\nu$) and then a boost in the direction

$$\mathbf{u} = \left(0, v_y\frac{\sqrt{(1-v_s)(1+v_s)}}{1-v_s v_x}, v_z\frac{\sqrt{(1-v_s)(1+v_s)}}{1-v_s v_x}\right) \rightarrow \hat{\Lambda}^\mu{}_\nu \ . \quad (2.25)$$

The four-velocity and the shock normal in the S-frame are then given by:

$$\hat{l}^\mu = (0,1,0,0) \ , \quad \hat{u}^\mu = \Gamma(v)(1,v,0,0) \ , \quad v = \frac{(v_s - v_x)}{\sqrt{(1-v_s v_x)^2 - (v_y^2+v_z^2)(1-v_s^2)}} \ . \quad (2.26)$$

Another way to reach the S-frame is by going from the LAB-frame to the fluid's rest-frame with a boost in the direction ($\mathbf{u} = (v_x,v_y,v_z) \rightarrow \Lambda'^\mu{}_\nu$) and from there to the shock-frame. Introduce the rotation tensors R_i , $i = x,y,z$ which rotate a four-vector around the i axis. The LAB-variables u^μ, b^μ and the shock normal $l^\mu = \Gamma(v_s)(v_s,1,0,0)$ are transformed to the fluid's rest-frame:

$$\begin{aligned} \bar{l}^\mu &= (R_z)^\mu{}_\xi (R_x)^\xi{}_\lambda \Lambda'^\lambda{}_\nu l^\nu = \Gamma(v)(v,-1,0,0) \\ \bar{u}^\mu &= (R_z)^\mu{}_\xi (R_x)^\xi{}_\lambda \Lambda'^\lambda{}_\nu u^\nu = (1,0,0,0) \\ \bar{b}^\mu &= (\bar{R}_x)^\mu{}_\eta (R_z)^\eta{}_\xi (R_x)^\xi{}_\lambda \Lambda'^\lambda{}_\nu b^\nu = (0,\bar{b}^1,\bar{b}^2,0) = \\ &= |b|(0,cos(\phi),sin(\phi),0) \ , \ |b| = \sqrt{b_\mu b^\mu} = \sqrt{(\bar{b}^1)^2+(\bar{b}^2)^2} \ , \end{aligned} \quad (2.27)$$

where the extra rotation ($\bar{R}_x$) applied on b^μ around the x-axis to get $\bar{b}^\mu$ has no effect on $\bar{l}^\mu, \bar{u}^\mu$. The different rotations are introduced to get b^μ in the form given in equation (2.27c). The angle ϕ represents the angle between the shock normal and the magnetic field in the rest frame of the fluid ahead of the shock. In a last step we transform to the S-frame by performing a Lorentz boost in the boost direction $\mathbf{u} = (0,-v,0,0) \rightarrow \bar{\Lambda}^\mu{}_\nu$. In the S-frame we have:

$$\begin{aligned} \hat{l}^\mu &= \bar{\Lambda}^\mu{}_\nu \bar{l}^\nu = (0,1,0,0) \\ \hat{u}^\mu &= \bar{\Lambda}^\mu{}_\nu \bar{u}^\nu = \Gamma(v)(1,v,0,0) \\ \hat{b}^\mu &= \bar{\Lambda}^\mu{}_\nu \bar{b}^\nu \quad (= \Gamma(v)(v|b|,|b|,0,0) \text{ if } \phi = 0) \ . \end{aligned} \quad (2.28)$$

2.2 Calculating LAB variables

To find the LAB variables from the shock solution proceeds as follows. Use the following relations resulting from equation (2.2):

$$[\tilde{B}u^\mu - a\tilde{b}^\mu] = 0 \ , \quad (2.29)$$

$$\left[nGau^\mu + \frac{n}{z}l^\mu + |\tilde{b}|^2\left(au^\mu + \frac{1}{2}l^\mu\right) - \tilde{B}\tilde{b}^\mu\right] = 0 \ . \quad (2.30)$$

In the LAB-frame $l^\mu = \Gamma(v_s)(v_s, 1, 0, 0)$. This system of eight equations can now be solved for the eight unknowns u^μ_+ and $\tilde{b}^\mu_+$. The above equations can be written in matrix form:

$$\begin{pmatrix} \tilde{B}_- & -a_- \\ a_- a_1 & -\tilde{B}_- \end{pmatrix} \begin{pmatrix} u^\mu_- \\ \tilde{b}^\mu_- \end{pmatrix} + a_2 \begin{pmatrix} 0^\mu \\ l^\mu \end{pmatrix} = \begin{pmatrix} \tilde{B}_+ & -a_+ \\ a_+ a_3 & -\tilde{B}_+ \end{pmatrix} \begin{pmatrix} u^\mu_+ \\ \tilde{b}^\mu_+ \end{pmatrix} + a_4 \begin{pmatrix} 0^\mu \\ l^\mu \end{pmatrix} , \tag{2.31}$$

where

$$a_1 = G_- + |\tilde{b}|^2_- , \quad a_2 = \frac{1}{z_-} + \frac{1}{2}|\tilde{b}|^2_- , \quad a_3 = n_+ G_+ + |\tilde{b}|^2_+ , \quad a_4 = \frac{n_+}{z_+} + \frac{1}{2}|\tilde{b}|^2_+ . \tag{2.32}$$

Solving for u^μ_+ and $\tilde{b}^\mu_+$ gives

$$\begin{pmatrix} u^\mu_+ \\ \tilde{b}^\mu_+ \end{pmatrix} = \frac{1}{D} \begin{pmatrix} (\tilde{B}_+ \tilde{B}_- - a_+ a_- a_1) u^\mu_- + (a_+ \tilde{B}_- - \tilde{B}_+ a_-) \tilde{b}^\mu_- \\ (a_+ \tilde{B}_- a_3 - \tilde{B}_+ a_- a_1) u^\mu_- + (\tilde{B}_+ \tilde{B}_- - a_+ a_- a_3) \tilde{b}^\mu_- \end{pmatrix} + \frac{(a_4 - a_2)}{D} \begin{pmatrix} a_+ l^\mu \\ \tilde{B}_+ l^\mu \end{pmatrix} , \tag{2.33}$$

where $D = \tilde{B}^2_+ - a^2_+ a_3$.

2.3 Characteristic speed versus shock speed

In the following we want to compare the shock speed with the characteristic speed after the shock (in the + region). A shock is compressible if $\lambda^+ > v_s > \lambda^-$. The λ corresponds to the fast or slow magneto-acoustic wave. The slow and fast magneto-acoustic waves travel at speeds which are the solution of equation (1.26), in the ideal gas case it transforms into:

$$nG\left(\frac{z}{\gamma} - \left(\frac{\gamma - 2}{\gamma - 1}\right)\right)(v^\lambda_\pm)^4 - \left(nG + |\tilde{b}|^2\left(\frac{z}{\gamma} + \frac{1}{\gamma - 1}\right)\right)(v^\lambda_\pm)^2(1 - (v^\lambda_\pm)^2) + \frac{\tilde{B}^2}{\phi^\mu \phi_\mu}(1 - (v^\lambda_\pm)^2)^2 = 0 , \tag{2.34}$$

and

$$v^\lambda_\pm = \frac{|u^\mu_\pm \phi_\mu|}{\sqrt{(g^{\mu\nu} + u^\mu_\pm u^\nu_\pm) l_\mu l_\nu}} = \left(\frac{\lambda^\pm - v^\pm_x}{1 - v^\pm_x \lambda^\pm} \text{ if } \phi^\mu = \Gamma(\lambda)(\lambda, 1, 0, 0)\right) . \tag{2.35}$$

The $\pm$ in $v^\lambda_\pm$ indicates if λ is calculated ahead or after the shock. The other quantities in equation (2.34) like $\tilde{B}, z$ are then also calculated in the $\pm$ region. In the following we take $\phi^\mu = \Gamma(\lambda)(\lambda, 1, 0, 0)$. To get a feeling for the meaning of $v^\lambda_\pm$ we take the limit $c \to \infty$. Then equation (2.34) approaches to:

$$\frac{nz}{\gamma}(v^\lambda_\pm)^4 - n(v^\lambda_\pm)^2 - \frac{z}{\gamma \rho_-}\mathbf{B} \cdot \mathbf{B}(v^\lambda_\pm)^2 + \frac{B^2_x}{\rho_-} = 0 , \tag{2.36}$$

where $v^\lambda_\pm \to \lambda^\pm - v^x_\pm$ and with the solution

$$(v^\lambda_\pm)^2 = \frac{1}{2}\left(c^2_s + \frac{\mathbf{B} \cdot \mathbf{B}}{\rho} \pm \sqrt{\left(c^2_s + \frac{\mathbf{B} \cdot \mathbf{B}}{\rho}\right)^2 - 4c^2_s \frac{B^2_x}{\rho}}\right) , \tag{2.37}$$

where $c^2_s = \frac{\gamma p}{\rho}$ represents the speed of sound. We now see that $v^\lambda_\pm = c_{s/f}$ corresponds to the fast/slow magneto-acoustic speeds in classical MHD with the eigenvalues $\lambda^{MHD}_{s,f} = v_x \pm c_{s/f}$. Because we work with relative quantities like $v^\lambda_\pm$ an equivalent expression for $\lambda^+ > v_s > \lambda^-$ is needed. For example in MHD the equivalent inequality is $\lambda^+ - v^-_x > v_s - v^-_x > \lambda^- - v^-_x$. In relativity we have to add velocities in a relativistic way. The relative shock speed $v^n_\pm$, relative to the fluid velocity $v^\pm_x$, is then

$$v^n_\pm = \frac{v_s - v^\pm_x}{1 - v^\pm_x v_s} \longrightarrow v^\pm_x = \frac{v_s - v^n_\pm}{1 - v^n_\pm v_s} . \tag{2.38}$$

If $n_+ \to 1$ (no shock) then $v_- \to v_-^\lambda$, the relative shock speed approaches the relative characteristic wave speed. The relative characteristic speed is given by equation (2.35), so

$$v_+^\lambda = \frac{\lambda^+ - v_x^+}{1 - v_x^+ \lambda^+} \longrightarrow \lambda^+ = \frac{v_x^+ + v_+^\lambda}{1 + v_x^+ v_+^\lambda} \ . \tag{2.39}$$

If $v_y = v_z = 0$ then $v_\pm^n$ (eq. 2.38) and $v_\pm$ (eq. 2.26) are the same. The shock relations (2.1) are solved given $z_-, a_-, |\tilde{b}|_-, \tilde{B}_-$. This gives us the freedom to choose $v_y^- = v_z^- = 0$ and $B_y^- = B_z^- = 0$ because we have nine unknowns and four determining equations. The four determining equations are the relations (2.3) connecting the quantities $z_-, a_-, |\tilde{b}|_-, \tilde{B}_-$ to $p_-, \rho_-, v_s, B_x^-, B_y^-, B_z^-, v_x^-, v_y^-, v_z^-$. If we choose $v_y^- = v_z^- = 0$ and $B_y^- = B_z^- = 0$ we also have, using equation (2.33), that $v_y^+ = v_z^+ = 0$ and $B_y^+ = B_z^+ = 0$. Therefore, we have that the $v_\pm$ in equation (2.26) is equivalent to $v_\pm^n$ in equation (2.38). If $c \to \infty$ then $v_+^\lambda = \lambda^+ - v_x^+$. But I want to compare (in the Newton limit) $v_-^n = v_s - v_x^-$ with $\hat{v}_+ = \lambda^+ - v_x^-$. The relativistic equivalent of $\hat{v}_+ = \lambda^+ - v_x^-$ is:

$$\hat{v}_+ = \frac{\lambda^+ - v_x^-}{1 - v_x^- \lambda^+} = \frac{v_+^n - v_+^\lambda - v_-^n (1 - v_+^\lambda v_+^n)}{v_-^n (v_+^n - v_+^\lambda) - 1 + v_+^\lambda v_+^n} \ . \tag{2.40}$$

If $c \to \infty$ then $\hat{v}_+ \to \lambda^+ - v_x^-$. The shock relations are solved for different v_-^n, resulting in n_+, z_+. The v_+^λ can now be calculated and v_+^n follows from $[\rho a] = 0$. In Figure 1 I have plotted $\hat{v}_+$ and v_-^n as a function of $1/n_+$. In this Figure only the slow magneto-acoustic wave/shock solutions are plotted. In Figure 1 the v_-^n curve cuts at $1/n_+ = 1$ the vertical axis, representing the different characteristic wave speeds in the S-frame. The lower cut represents the slow magneto-acoustic wave speed and the upper cut represents the Alfvén wave speed. The region where the shock is compressive can now easily be determined as the region where $\hat{v}_+ > v_-^n > v_-^\lambda$ holds. The shock curve in Figure 1 represents a compressive shock from the point $(1.0, 0.247)$ to the point $(0.553, 0.488)$. In MHD, where a similar curve exists, there are authors like Falle [3] which claim that already the point where $v_n^- > v_{\text{Alfvén}}^\lambda$ represents an over-compressive[1] shock and is not allowed. In our case, this means that the shock curve in Figure 1 represents a shock until the point $(0.440, 0.471)$. After this point the relative slow shock speed v_-^n is faster than the relative Alfvén shock speed $v_{\text{Alfvén}}^\lambda$. For more details concerning this topic the reader is referred to the papers of Wu [12], Myong [8] and Torrilhon [11].

2.4 Results

The shock relations (2.9,2.10) can be solved for the slow/fast magneto-acoustic shocks with the method described in Section 2. To eliminate certain non-physical (entropy violating) solutions the following conditions $p_+ > p_-$, $\rho_+ > \rho_-$, $z_+ < z_-$ and $a_-/a_+ > 1$ from Majorana [7] must hold. The quantities n_+, z_+ can be plotted as a function of v_- if the quantities a_-, $|\tilde{b}|_-$, $\tilde{B}_-$, z_- and $n_- = 1$ ahead of the shock are known. As already mentioned we are open to choose our reference frame because scalar quantities are frame invariant. For convenience sake we calculate $\tilde{B}_-$ in the fluid's rest-frame ahead of the shock and a_- in the S-frame, see Section 2.1. In the S-frame we have $\hat{u}^\mu = \Gamma(v_-)(1, v_-, 0, 0)$ and $\hat{l}^\mu = (0, 1, 0, 0)$. In the fluid's rest-frame we have $\bar{b}_-^\mu = |b|_-(0, cos(\phi), sin(\phi), 0)$ and $\bar{l}^\mu = \Gamma(v_-)(v_-, 1, 0, 0)$. The angle ϕ represents the angle between the shock normal and the magnetic field in the rest frame of the fluid ahead of the shock. So,

$$a_- = \Gamma(v_-) v_- \ , \quad \tilde{B}_- = \Gamma(v_-) |\tilde{b}|_- cos(\phi) \ . \tag{2.41}$$

In Figure 2 the results for $z_- = 10, |\tilde{b}|_- = 1$ are shown for different ϕ as a function of v_-. The points where the line $n_+ = 1$ crosses the curve representing n_+ as a function of v_- correspond, for increasing

[1] Over-compressive shock with shock speed v_s^i is defined as $\lambda_j^+ > \lambda_i^+ > v_s^i > \lambda_j^- > \lambda_i^-$, $j > i > k$ and the indeces i, j, k indicate the wave family. A compressive shock is defined as: $\lambda_j^\pm > \lambda_i^+ > v_s^i > \lambda_i^- > \lambda_k^\pm$.

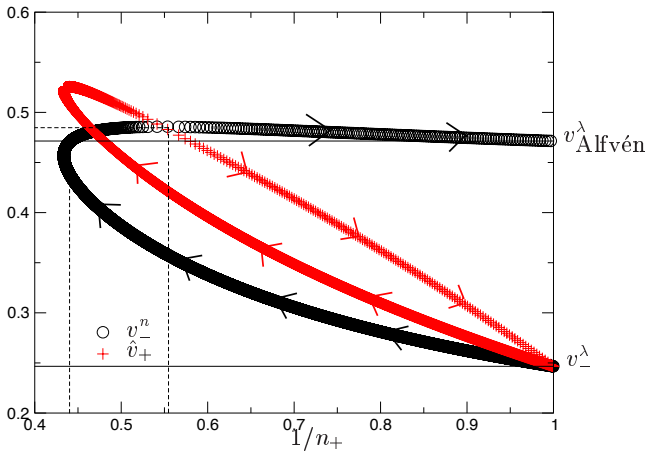

Figure 1: *Plot of* $\hat{v}_+$ *and* v^n_- *as function of* $1/n_+$ *for* $\phi = 45^o$, $z_- = 10$ *and* $|\tilde{b}|_- = 1$.

v_-, to the slow magneto-acoustic wave speed, the Alfvén wave speed and the fast magneto-acoustic wave speed. In the case of $\phi = 90^o$ there is only a shock curve corresponding to a fast magneto-acoustic wave. Parts of the slow shock curve do not represent shocks as was explained in the Section 2.3.

3. Alfvén shock

In the following we treat in more detail the Alfvén shock in the shock-frame. We follow the work of Komissarov [5]. In the shock frame $l^\mu = (0,1,0,0)$, $a = u^1$, $B = b^1$. The Alfvén shock relations in the shock frame look like:

$$\begin{aligned} &[u^1] = 0 \\ &[b^1] = 0 \\ &[|b|^2] = 0 \\ &[u^\mu] = \chi\,[b^\mu] \ , \ \chi = \tfrac{u^1}{b^1} \ . \end{aligned} \tag{3.1}$$

From equation $(3.1)^4$ we find:

$$u^\mu_+ = u^\mu_- + \chi[b^\mu] \ , \tag{3.2}$$

and this expression can be substituted in the algebraic constraint $u_\mu b^\mu = 0$, resulting in:

$$b^0_+ = a_y b^2_+ + a_z b^3_+ + c \tag{3.3}$$

where

$$a_y = \frac{u^2_- - \chi b^2_-}{u^0_- - \chi b^0_-} \ , \ a_z = \frac{u^3_- - \chi b^3_-}{u^0_- - \chi b^0_-} \ , \ c = \frac{\chi |b|^2_-}{u^0_- - \chi b^0_-} \ . \tag{3.4}$$

The shock relation (3.1c) gives

$$-(b^0_+)^2 + (b^2_+)^2 + (b^3_+)^2 = d \ , \quad d = |b|^2_- - (b^1_-)^2 \ . \tag{3.5}$$

The expression for b^0_+, equation (3.3), can be substituted in equation (3.5).

$$a_{11}(b^2_+)^2 + 2a_{12}b^2_+ b^3_+ + a_{22}(b^3_+)^2 + 2a_{13}b^2_+ + 2a_{23}b^3_+ + a_{33} = 0 \ , \tag{3.6}$$

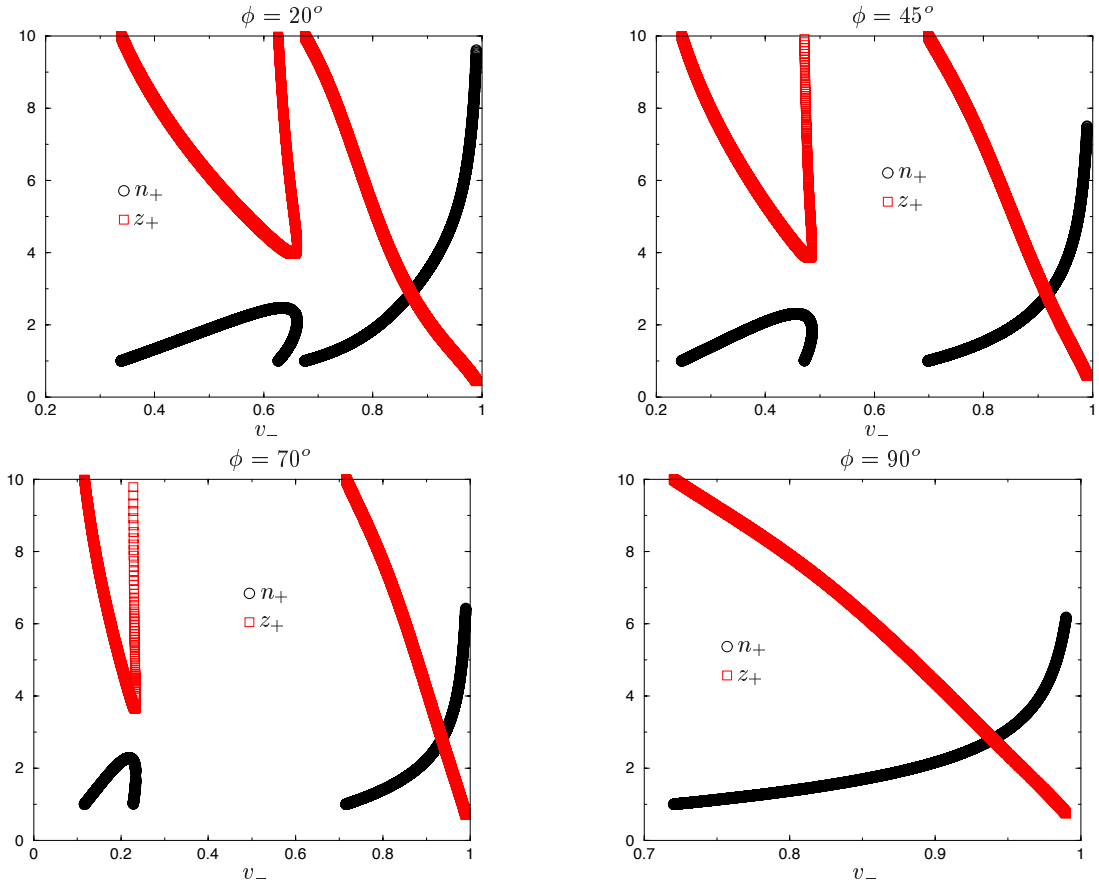

Figure 2: *Shock solutions for different* ϕ *as function of* v_- *for* $z_- = 10$ *and* $|\tilde{b}|_- = 1$.

where

$$\begin{aligned} a_{11} &= 1 - a_y^2 & a_{22} &= 1 - a_z^2 \\ a_{33} &= -(c^2 + d) & a_{12} &= -a_y a_z \\ a_{13} &= -c a_y & a_{23} &= -c a_z \ . \end{aligned} \tag{3.7}$$

In Komissarov [5] it is shown that the conic (3.6) is an ellipse. The origin of the ellipse is located at

$$(b_c^2, b_c^3) = \frac{c}{D}(a_y, a_z) \ , \quad D = a_{11}a_{22} - 2a_{12} \ . \tag{3.8}$$

The minor and major axis are respectively

$$l_a^2 = -\frac{A}{D} \ , \quad l_a^2 = -\frac{A}{D^2} \ , \tag{3.9}$$

and the angle between the major axis and the y-axis is given by

$$\psi = \arctan\left(\frac{a_z}{a_y}\right) \ . \tag{3.10}$$

The ellipse can also be described by

$$\begin{aligned} b_+^2 &= b_c^2 + \sin(\psi) l_a \cos(\theta) + \cos(\psi) l_b \sin(\theta) \\ b_+^3 &= b_c^3 - \cos(\psi) l_a \cos(\theta) + \sin(\psi) l_b \sin(\theta) \ . \end{aligned} \tag{3.11}$$

and the free parameter θ. In Figure 3 a typical solution for b_+^2 and b_+^3 is shown.

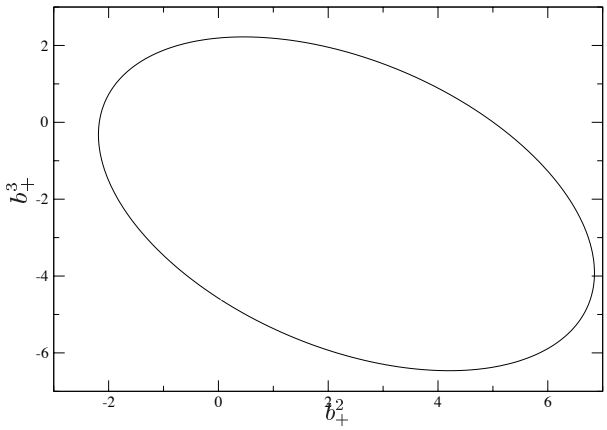

Figure 3: *Plot of allowed combinations of* b_+^2 *and* b_+^3 *in the case of an Alfvén shock with* $b_-^\mu = (0.1, 1.0, -1.5, 1.5)$ *and* $u_-^\mu = (1.0, 0.3, 0.1, -0.05)$.

4. Exact Riemann solver for shocks only

In the last sections it is explained how the state behind a shock can be calculated if the state ahead of a shock is known. The unknown quantities are the four different shock speeds and the two parameters θ^- (θ^+) describing the left (right) going Alfvén shock. In Figure 4 the different shocks occurring in RMHD are plotted together with the symbols used to describe the different shocks/waves and the symbols used to indicate the different regions. The $-(+)$ sign corresponds to a left (right) going shock. The six shock relations at the contact discontinuity (CD) are:

$$\begin{aligned} &p_3 - p_4 = 0 \\ &v_x^3 - v_x^4 = 0 \\ &v_y^3 - v_y^4 = 0 \\ &v_z^3 - v_z^4 = 0 \\ &B_y^3 - B_y^4 = 0 \\ &B_z^3 - B_z^4 = 0 \, . \end{aligned} \tag{4.1}$$

So, we have six unknowns and six (nonlinear)equations. This can be written in a more compact form:

$$\mathbf{F}(\mathbf{X}, \theta^-, \theta^+) = 0 \, , \tag{4.2}$$

where $\mathbf{X}$ is a parameterization of the four different shock speeds.

A standard nonlinear solver from the NAG library (C05NBF) is used to solve the system (4.1). In the following the vector $\mathbf{X} = (x_1, x_2, x_3, x_4)^T$ is connected to the shock speeds. In the LAB-frame we have the following characteristic wave speeds: $\lambda_f^{(i)}, \lambda_A^{(i)}, \lambda_s^{(i)}$. The (i) indicates in which region $\lambda^{(i)}$ is calculated. The $v_{f,s}^{\pm}$ represent the different shock speeds. In this part of the research we focus on shocks only. The shock speeds are restricted to certain values:

$$\begin{aligned} &\lambda_f^{(0)} < v_f^+ < 1 \\ &-1 < v_f^- < \lambda_f^{(7)} \\ &\lambda_s^{(2)} < v_s^+ < \lambda_A^{(2)} \\ &\lambda_s^{(5)} < v_s^- < \lambda_A^{(5)} \, . \end{aligned} \tag{4.3}$$

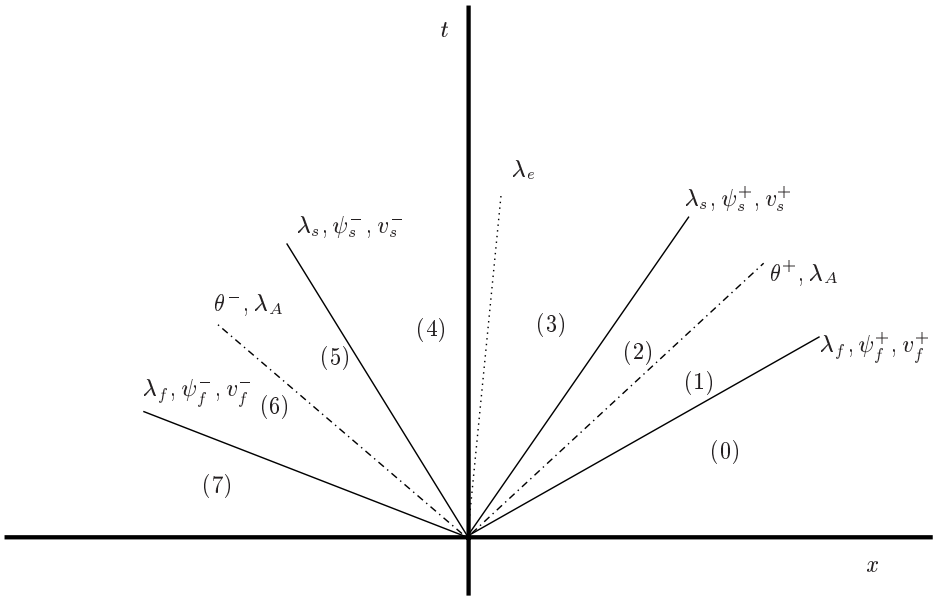

Figure 4: *Plot of the different shocks occurring in RMHD and the symbols used in connection to these shocks and waves.*

In general a standard solver can not put restrictions on the domain of $\mathbf{X}$. With the following transformations on $\mathbf{X}$ we ensure that (4.3) holds for $\mathbf{X} \in I\!R$. For the fast shock we take

$$\psi_f^{\pm} = \frac{1}{2} + \frac{1}{\pi} tan^{-1}(x) \tag{4.4}$$

where for the right (left) going shock $x = x_1$ ($x = x_3$). Using the relativistic addition law we find for the left(right) going fast shock:

$$v_f^+ = \frac{\lambda_f^{(0)} + \psi_f^+}{1 + \lambda_f^{(0)} \psi_f^+} \ , \quad v_f^- = \frac{\lambda_f^{(7)} - \psi_f^-}{1 - \lambda_f^{(7)} \psi_f^-} \ . \tag{4.5}$$

For the slow shocks we take

$$\psi_s^{\pm} = \frac{1}{2} \psi_{max}^{\pm} + \frac{\psi_{max}^{\pm}}{\pi} tan^{-1}(x) \ , \tag{4.6}$$

where for the right (left) going shock $x = x_2$ ($x = x_4$). To ensure that inequalities (4.3c) and (4.3d) hold we take:

$$\psi_{max}^+ = \frac{\lambda_A^{(2)} - \lambda_s^{(2)}}{1 - \lambda_A^{(2)} \lambda_s^{(2)}} \ , \quad \psi_{max}^- = \frac{\lambda_s^{(5)} - \lambda_A^{(5)}}{1 - \lambda_A^{(5)} \lambda_s^{(5)}} \ . \tag{4.7}$$

Using the relativistic addition law we find for the left(right) going slow shock:

$$v_s^+ = \frac{\lambda_s^{(2)} + \psi_s^+}{1 + \lambda_s^{(2)} \psi_s^+} \ , \quad v_s^- = \frac{\lambda_s^{(5)} - \psi_s^-}{1 - \lambda_s^{(5)} \psi_s^-} \ . \tag{4.8}$$

We also put a restriction on $\theta^{\pm}$ to ensure that $0 \leq \theta^{\pm} \leq 2\pi$.

$$\theta^{\pm} \rightarrow \pi + 2 tan^{-1}(\theta^{\pm}) \ . \tag{4.9}$$

All the ingredients to solve equation (4.2) are now present. If the left and right states of the Riemann problem are given the solution can be calculated. The non-linear system solver needs an initial guess for the vector $\mathbf{X}$. This initial guess is used to calculate with the help of the slow/fast and Alfvén shock solution the differences (4.1) at the CD which are used to correct the vector $\mathbf{X}$. In Table 1 the initial conditions of Problem 0 and the final results are shown. The starting vector is ($\mathbf{X} = (0.1, 0.1, 0.1, 0.1)$, $\theta^{\pm} = 0.0$). After 76 iterations $|\mathbf{F}(\mathbf{X}, \theta^-, \theta^+)| < 1 \cdot 10^{-9}$ and ($\mathbf{X} = (-1.6564, -28.40, -2.1875, 0.5566)$, $\theta^- = 0.5148$, $\theta^+ = 1.1156$). The model Problem 4 of Balsara

	State 7	State 6	State 5	State 4	State 3	State 2	State 1	State 0
p	0.1	0.3570	0.3570	1.7914	1.7914	1.7758	1.7758	1.0
ρ	1.08	1.7585	1.7585	4.2290	1.4130	1.4056	1.4056	1.0
v_x	0.4	-0.1197	-0.4478	-0.3599	-0.3599	-0.3625	-0.3637	-0.55
v_y	0.3	-0.0846	-0.4319	-0.1047	-0.1047	-0.1017	-0.1223	-0.2
v_z	0.2	0.6504	0.3340	0.1680	0.1680	0.1661	0.1368	0.2
B_x	2.0	2.0	2.0	2.0	2.0	2.0	2.0	2.0
B_y	0.3	-0.6922	-1.6275	-1.0860	-1.0860	-1.0924	-1.0212	-0.7
B_z	0.3	2.0094	0.8692	0.6464	0.6464	0.6504	0.7468	0.5
v_s	-	-0.7379	-0.7318	-0.6211	-0.3599	0.1593	0.2361	0.5259

Table 1: *Initial state of Problem 0 and the intermediate states calculated with the exact Riemann solver.*

[2] contains only shocks and is also used to demonstrate the exact Riemann solver. In Table 2 the results for Problem 4 are summarized. The starting vector is ($\mathbf{X} = (0.1, 0.1, 0.1, 0.1)$, $\theta^{\pm} = 0.0$). After 54 iterations $|\mathbf{F}(\mathbf{X}, \theta^-, \theta^+)| < 1 \cdot 10^{-9}$ and ($\mathbf{X} = (5.2778, 30.0443, 5.2778, 30.0443)$, $\theta^- = -1.0$, $\theta^+ = 1.0$). In general, small changes in the starting vector $\mathbf{X}$ do not change the convergent behavior of

	State 7	State 6	State 5	State 4	State 3	State 2	State 1	State 0
p	0.1	855.7777	855.7777	1146.4811	1146.4811	855.7777	855.7777	0.1
ρ	1.0	51.7461	51.7461	61.4745	61.4745	51.7461	51.7461	1.0
v_x	0.999	0.0441	0.0441	0.0	0.0	0.0441	0.0441	-0.999
v_y	0.0	0.0326	0.0326	-0.2877	-0.2877	0.0326	0.0326	0.0
v_z	0.0	0.0326	0.0326	-0.2877	-0.2877	0.0326	0.0326	0.0
B_x	10.0	10.0	10.0	10.0	10.0	10.0	10.0	10.0
B_y	7.0	16.6785	16.6785	0.0	0.0	-16.6785	-16.6785	-7.0
B_z	7.0	16.6785	16.6785	0.0	0.0	-16.6785	-16.6785	-7.0
v_s	-	-0.68029	-0.14808	-0.14797	0.0	0.14797	0.14808	0.68029

Table 2: *Initial state of Problem 4 from Balsara [2] and the intermediate states calculated with the exact Riemann solver.*

the non-linear system solver. However, too large changes in the starting vector $\mathbf{X}$ result in a non-convergent behavior of the non-linear system solver. The solver converges to an $\mathbf{X}$ which is not a solution of $\mathbf{F}(\mathbf{X})$. In the next section the results of the exact Riemann solver are compared with the results obtained with the Lax-Friedrichs scheme.

5. Numerical solutions

In the following the solutions of certain Riemann problems given in Table (3) are computed with the Lax-Friedrichs (LF) scheme and to obtain second order in space a MINMOD reconstruction procedure for the primitive variables is used. Therefore, the system (1.27) is solved numerically on the domain $x \in [0, 1]$ and at $x = 0.5$ the domain is split in a Left(Right) region to define the Left(Right) initial

	Problem 1		Problem 2		Problem 3		Problem 4		Problem 5	
	L	R	L	R	L	R	L	R	L	R
p	1.0	0.1	30.0	1.0	1000.0	0.1	0.1	0.1	0.95	1.0
ρ	1.0	0.125	1.0	1.0	1.0	1.0	1.0	1.0	1.08	1.0
v_x	0.0	0.0	0.0	0.0	0.0	0.0	0.999	-0.999	0.4	-0.45
v_y	0.0	0.0	0.0	0.0	0.0	0.0	0.0	0.0	0.3	-0.2
v_z	0.0	0.0	0.0	0.0	0.0	0.0	0.0	0.0	0.2	0.2
B_x	0.5	0.5	5.0	5.0	10.0	10.0	10.0	10.0	2.0	2.0
B_y	1.0	-1.0	6.0	0.7	7.0	0.7	7.0	-7.0	0.3	-0.7
B_z	0.0	0.0	6.0	0.7	7.0	0.7	7.0	-7.0	0.3	0.5

Table 3: *Left and right initial values for Riemann Problems, from Balsara [2].*

conditions. A mesh is defined in the (x,t)-plane in order to discretize equation (1.27). The points on the mesh are at locations $(x_i = i\Delta x,\ t^n = n\Delta t)$ with $i = 0,..,N_x$ and $n = 0,..,N_t$. The discrete values of $\mathbf{U}(x,t)$ at $(i\Delta x,\ n\Delta t)$ will be denoted by $\mathbf{U}_i^n$. The conserved variables $\mathbf{U}(x,t)$ are advanced in time in the following way:

$$\mathbf{U}_i^{n+1} = \mathbf{U}_i^n + \frac{\Delta t}{\Delta x}\left(\mathbf{F}_{i-\frac{1}{2}} - \mathbf{F}_{i+\frac{1}{2}}\right), \tag{5.1}$$

where $\mathbf{F}_{i+\frac{1}{2}}$ is the flux through the cell face located at $x_{i+\frac{1}{2}}$. To ensure that no waves interact within a cell, the time step must satisfy the condition:

$$\Delta t = \sigma\frac{\Delta x}{S_{max}^n}\ ,\ 0 < \sigma \leq 1\ , \tag{5.2}$$

where σ is the Courant number, S_{max}^n the largest signal velocity in the domain at a certain time step t^n and $\Delta x = 1.0/N_x$ is the grid spacing used. In all following calculations we take for simplicity $S_{max}^n = 1$, the speed of light. The LF flux is computed according to:

$$\mathbf{F}_{i+\frac{1}{2}} = \frac{1}{2}\left(\mathbf{F}_i^n + \mathbf{F}_{i+1}^n - C_{i+\frac{1}{2}}^{max}(\mathbf{U}_{i+1}^n - \mathbf{U}_i^n)\right)\ , \tag{5.3}$$

where

$$C_{i+\frac{1}{2}}^{max} = max[C_i^{max}, C_{i+1}^{max}]\ ,\ C_i^{max} = (max_p[|\lambda_p|])_i\ . \tag{5.4}$$

The eigenvalues for the magneto-sonic waves are given by solving the quartic (1.26) with the NAG library routine CO2ALF.

To find the primitive variables from the conservative variables one nonlinear equation must be solved as is the case in SRHD. We have the conserved quantities, the vector $\mathbf{U}$ in equation (1.28),

$$\begin{aligned} D &= \rho\Gamma \\ \mathbf{S} &= (\rho h\Gamma^2 + \mathbf{B}^2)\mathbf{v} - \mathbf{B}(\mathbf{v}\cdot\mathbf{B}) \\ \tau &= \rho h\Gamma^2 + \tfrac{1}{2}\mathbf{B}^2 - p + \tfrac{1}{2}(\mathbf{B}^2\mathbf{v}^2 - (\mathbf{v}\cdot\mathbf{B})^2)\ . \end{aligned} \tag{5.5}$$

Define

$$\begin{aligned} \mathbf{S}^2 &= \mathbf{S}\cdot\mathbf{S} = (\rho h\Gamma^2)^2\mathbf{v}^2 + (2\rho h\Gamma^2 + \mathbf{B}^2)(\mathbf{B}^2\mathbf{v}^2 - (\mathbf{v}\cdot\mathbf{B})^2) \\ \Pi &= \mathbf{S}\cdot\mathbf{B} = \rho h\Gamma^2(\mathbf{v}\cdot\mathbf{B})\ . \end{aligned} \tag{5.6}$$

Introduce

$$x = \rho h\Gamma^2\ , \tag{5.7}$$

then, rearranging the expression for the enthalpy $h = (e + p)/\rho$ and using the state equation (1.20) gives:

$$p = \frac{1}{\bar{\gamma}}(\rho h - \rho) = \frac{1}{\bar{\gamma}}(\frac{x}{\Gamma^2} - \frac{D}{\Gamma}) \ , \tag{5.8}$$

and

$$(\mathbf{v} \cdot \mathbf{B}) = \frac{\Pi}{x} \ . \tag{5.9}$$

From equations (5.6a) and (5.9) an expression for $\mathbf{v}^2$ follows

$$\mathbf{v}^2 = \frac{\mathbf{S}^2 + 2\Pi^2/x + \Pi^2\mathbf{B}^2/x^2}{(x + \mathbf{B}^2)^2} \ . \tag{5.10}$$

The expression for τ, equation (5.5c) can be simplified to an expression containing only one unknown:

$$f(x) = x - \frac{\gamma - 1}{\gamma}\left(\frac{x}{\Gamma(x)^2} - \frac{D}{\Gamma(x)}\right) - \frac{1}{2}\left(\frac{\mathbf{B}^2}{\Gamma(x)^2} + \frac{(\mathbf{S} \cdot \mathbf{B})^2}{x^2}\right) = \tau - \mathbf{B}^2 \ . \tag{5.11}$$

With a Newton-Raphson procedure this equation in x can be solved. It uses the Jacobian $\frac{df}{dx}$:

$$\begin{array}{l} \frac{d\Gamma}{dx} = -\Gamma(x)^3 \frac{(\mathbf{S}\cdot\mathbf{B})^2(3x^2+3x\mathbf{B}^2+\mathbf{B}^4)+\mathbf{S}^2x^3}{x^3(x+\mathbf{B}^2)^3} \\ \frac{df}{dx} = 1 + \frac{(\mathbf{S}\cdot\mathbf{B})^2}{x^3} - \frac{1}{\bar{\gamma}\Gamma^2} + \frac{d\Gamma}{dx}\left(\frac{2x}{\bar{\gamma}\Gamma^3} - \frac{D}{\bar{\gamma}\Gamma^2} + \frac{\mathbf{B}^2}{\Gamma^3}\right) \end{array} \ . \tag{5.12}$$

In Koldoba [4] it is argued that $f(x)$ is monotonously increasing. For a positive pressure we must have $\frac{x^2}{\Gamma^2} \geq D^2$. This is true for $x \geq \bar{x}$ where $\bar{x}$ is the maximal real root of $\frac{x^2}{\Gamma^2} = D^2$. So there exists a solution if $f(\bar{x}) \leq \tau - \mathbf{B}^2$.

The LF-scheme is used to compute Problem 1 and 3 in Table 3. The results are plotted in Figures 5 and 6, respectively and show good agreement with the results obtained with the more advanced numerical method given in Balsara [2]. In Figure 5 we can distinguish the seven waves/shocks occurring in RMHD. From left to right we have: rarefaction wave, compound wave (this is a combination of a (Alfvén) shock and a rarefaction wave), contact discontinuity, slow shock, Alfvén shock and a fast shock. The Figure also shows the behavior of the solution under mesh refinement. Figure 6 shows the RMHD equivalent of the ultra-relativistic shock already encountered in SRHD, see Odyck [9].

5.1 Comparing exact with LF solution

Figures 7 and 8 show the exact and LF-solution of Problem 0 and Problem 4, respectively. They show good agreement between the exact and the numerical solution. This is quantified in Table 4 where the L_1 norm, defined as

$$||y^n||_1 = \Delta x \sum_{i=1}^{M} |y_i^n| \ , \tag{5.13}$$

is given and, in our case, y_i^n represents p_i^n or ρ_i^n. The quantities between the brackets in Table 4 are defined as

$$\frac{||y^n - y||_1^{2\Delta x}}{||y^n - y||_1^{\Delta x}} \ , \tag{5.14}$$

and are an indication of the discretization order. For a first order scheme they should approach the value two. The values in Table 4 show first order behavior as is expected for a second order scheme (in space) in the presence of shocks.

	Problem 0		Problem 4	
Δx	$\|\|p^n - p\|\|_1$	$\|\|\rho^n - \rho\|\|_1$	$\|\|p^n - p\|\|_1$	$\|\|\rho^n - \rho\|\|_1$
0.0025	0.01800	0.06647	10.91	0.7765
0.00125	0.01026 (1.8)	0.03846 (1.7)	6.45 (1.7)	0.4437 (1.8)
0.000625	0.00573 (1.8)	0.02304 (1.7)	4.13 (1.6)	0.2812 (1.6)
0.0003125	0.00271 (2.1)	0.01289 (1.8)	2.12 (2.0)	0.1434 (2.0)
0.00015625	0.001563 (1.7)	0.007597 (1.7)	1.06 (2.0)	0.0739 (1.9)

Table 4: *The L_1 norm as function of Δx for Problem 0 (at $T = 0.4$) and Problem 1 (at $T = 0.6$).*

6. Conclusions

It is shown how the RMHD equations are derived from the Maxwell equations and the laws of conservation of energy, momentum and number of particles under the assumption of infinite conductivity. The jump conditions are studied and a detailed description is given of a solution method to solve the shock relations for the slow and fast magneto-acoustic shocks. A method is developed to solve the RMHD Riemann problem in the case of shocks only. The exact solutions are compared with the numerical solutions calculated with the Lax-Friedrichs method. The results show that the Lax-Friedrichs solution converges to the exact solution but more important it indicates that the exact Riemann solver works.

References

1. A.M. Anile, *Relativistic fluids and magneto-fluids*, Cambridge University Press (1989).
2. D. Balsara, Total variation diminishing scheme for relativistic magneto-hydrodynamics, *ApJS*, 132:83-101, (2001).
3. S.A.E.G. Falle and S.S. Komissarov, On the inadmissibility of non-evolutionary shocks, *J. Plasma Phys.*, **65**(Part 1), 29-58 (2001).
4. A.V. Koldoba, O.A. Kuznetsov and G.V. Ustyugova, An approximate Riemann solver for relativistic magneto-hydrodynamics, *Mon. Not. R. Astron. Soc.*, **333**, 932-942 (2002).
5. S.S. Komissarov, On the properties of Alfvén waves in relativistic magnetohydrodynamics, *Phys. Let. A*, **232**, 435-442 (1997).
6. A. Lichnerowicz, *Relativistic hydrodynamics and magnetohydrodynamics*, W.A. Benjamin, Inc. New York (1967).
7. A. Majorana and A.M. Anile, Magnetoacoustic shock waves in a relativistic gas, *Phys. Fluids*, **30**(10), 3045-3049 (1987).
8. R.S. Myong, Analytical results on MHD intermediate shocks, *Geophys. Res. Lett.*, **24**(No. 22), 2929-2932 (1997).
9. D.E.A. van Odyck, Review of numerical special relativistic hydrodynamics, *Report MAS-R0212*, CWI, Amsterdam (2002).
10. B.T. Smith, ZERPOL: A zero finding algorithm for polynomials using Laguerre's method, Technical Report, Department of computer science, University of Toronto, Canada (1967).
11. M. Torrilhon, Exact solver and Uniqueness conditions for Riemann problems of ideal magnetohydrodynamics, *Research report No. 2002-06*, Seminar für Angewandte Mathematik, Eidgenössische Technische Hochschule, Zürich Switzerland (2002).
12. C.C. Wu, The MHD intermediate shock interaction with an intermediate wave: are intermediate shocks physical?, *J. Geophys. Res.*, **93**(No. A2), 987-990 (1988).

Table of Contents

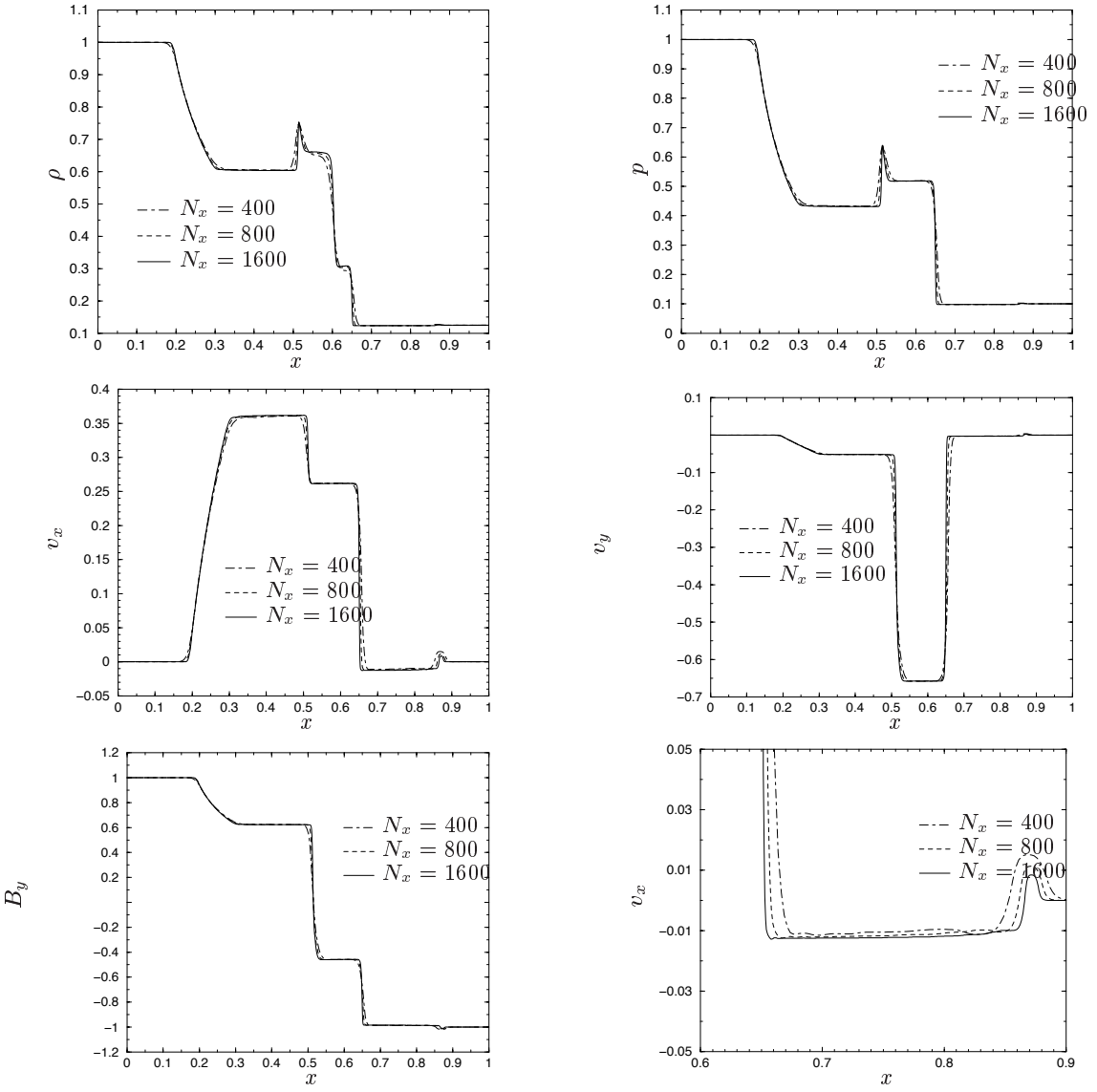

Figure 5: *LF with MINMOD solution for Problem 1 from Balsara [2].* $T = 0.4$, $\sigma = 0.1$.

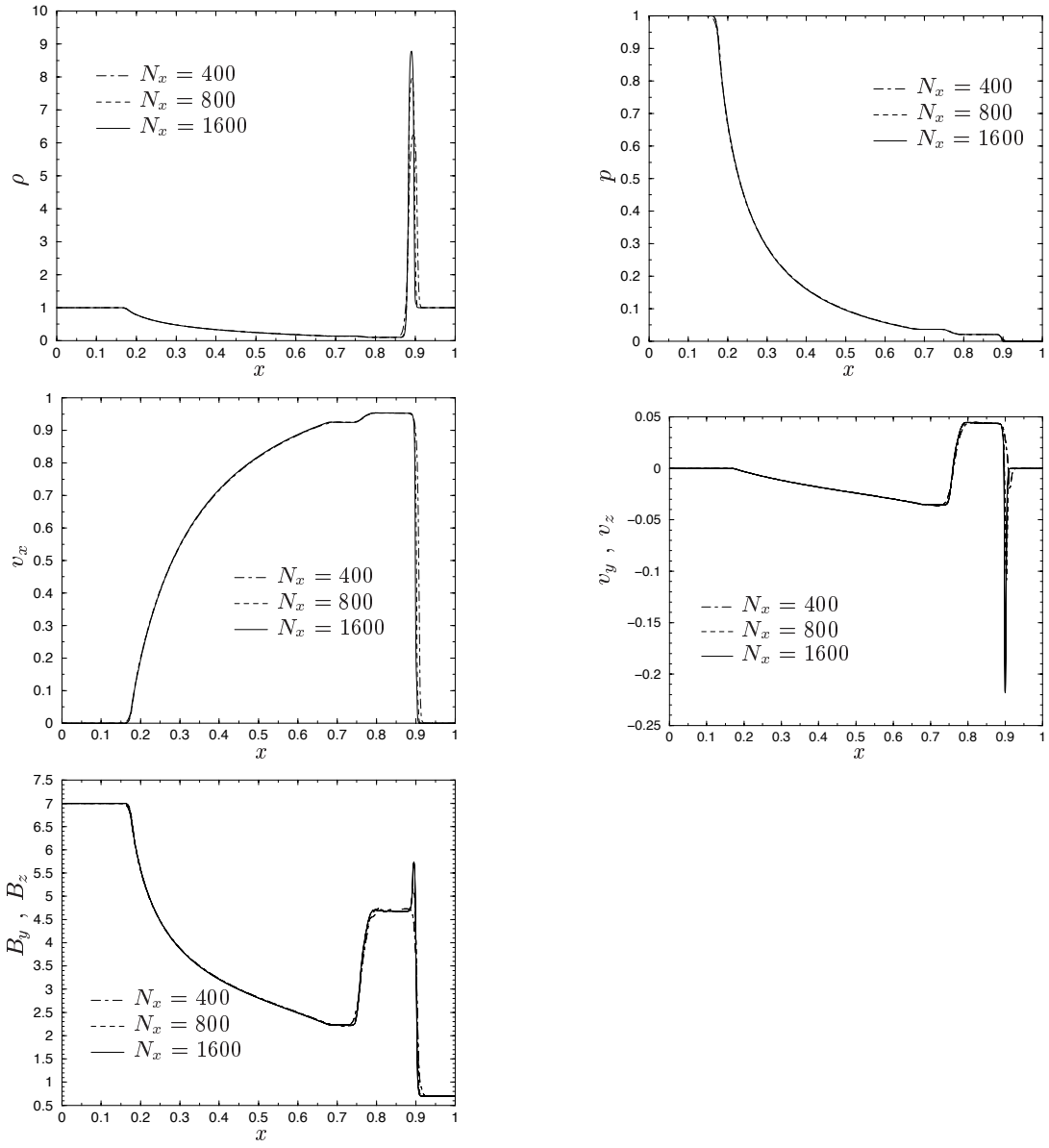

Figure 6: *LF with MINMOD solution for Problem 3 from Balsara [2]. $T = 0.4$, $\sigma = 0.2$. If $N_x = 1600$ then $\sigma = 0.1$.*

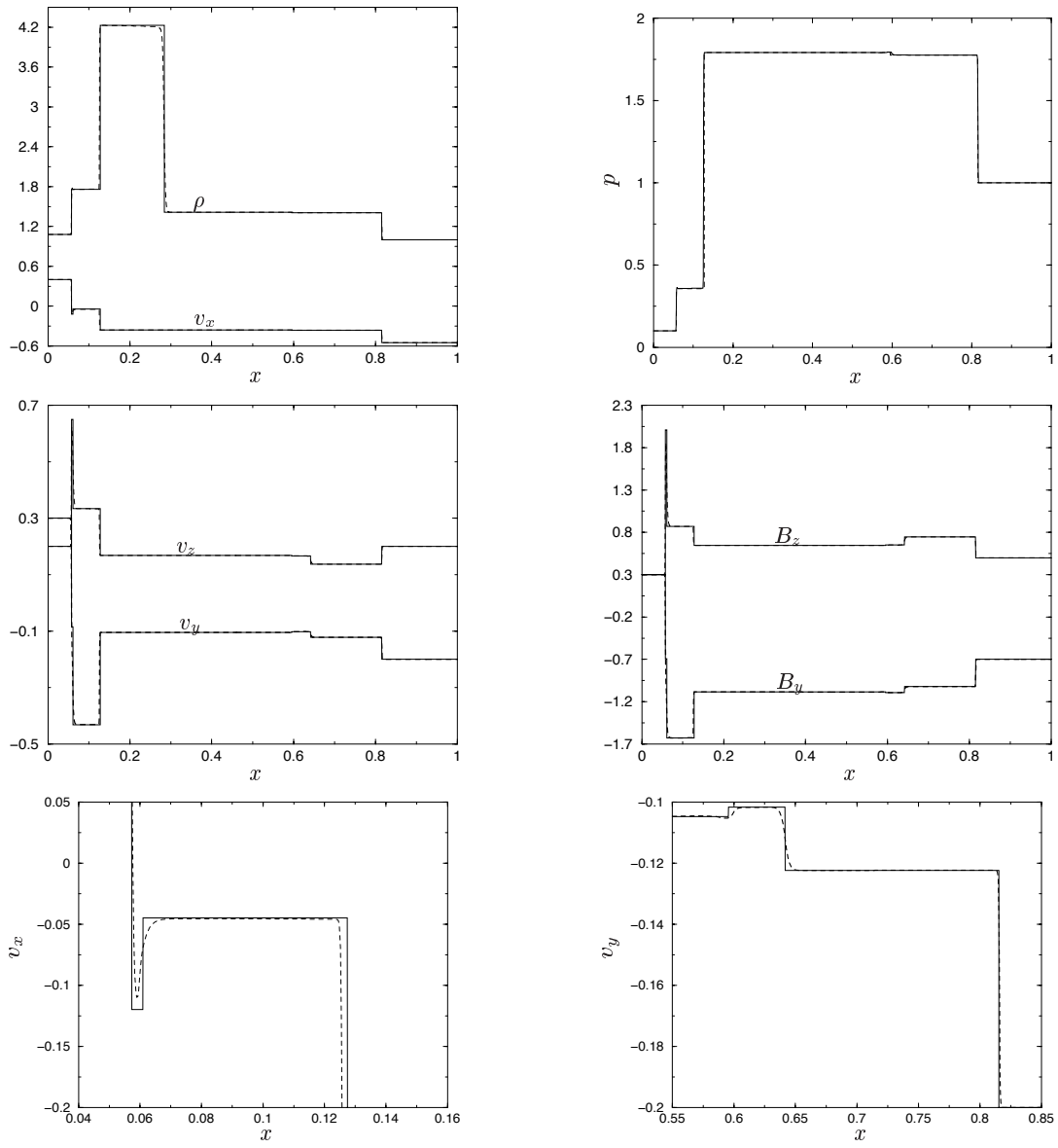

Figure 7: *LF with Woodward limiter for problem given in Table 1.* $T = 0.6$, $\sigma = 0.1$, $N_x = 3200$.

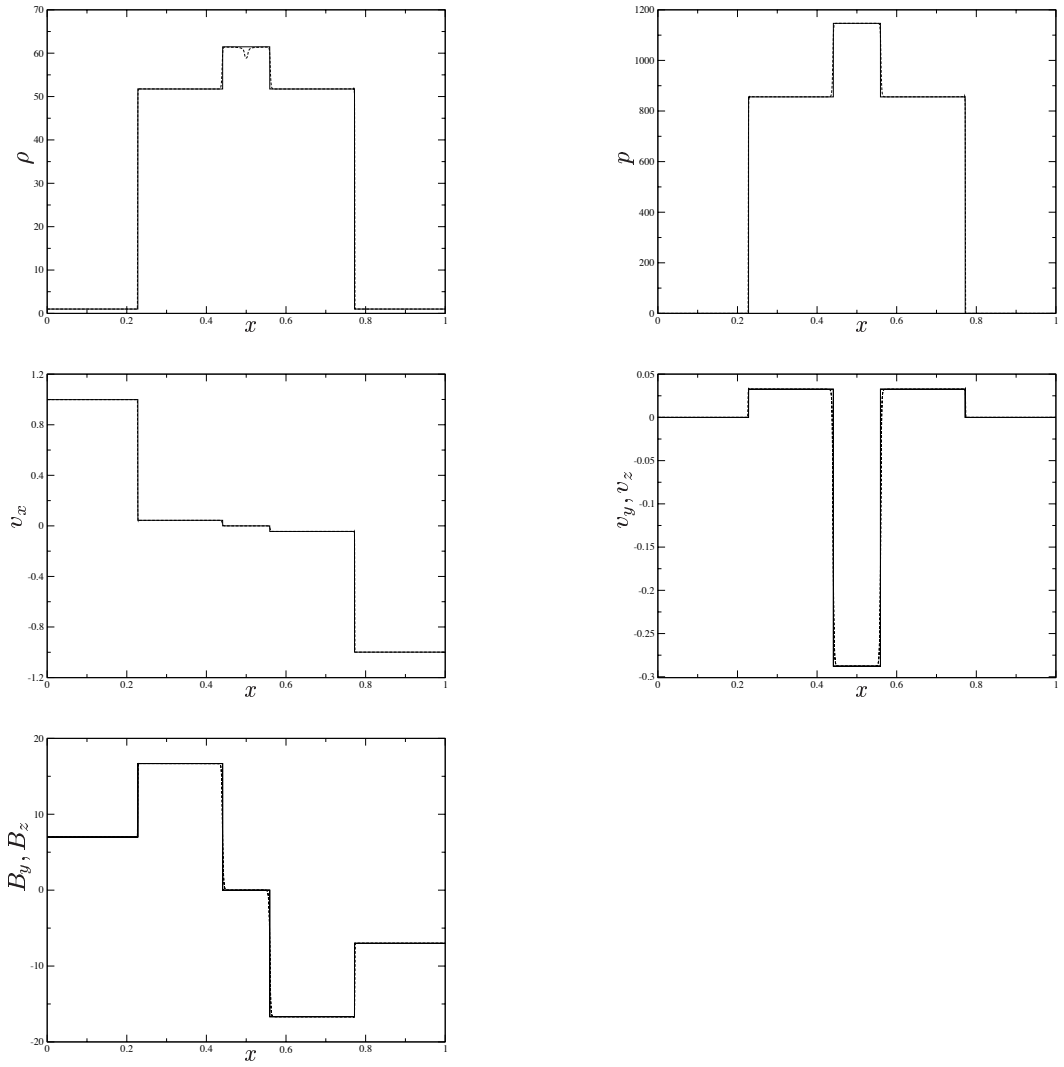

Figure 8: *LF with MINMOD limiter for problem given in Table 2.* $T = 0.4$, $\sigma = 0.1$, $N_x = 3200$.